J Therm Anal Calorim (2012) 108:1183–1188
DOI 10.1007/s10973-011-1660-0

Thermal behaviour of fumaric acid, sodium fumarate and its compounds with light trivalent lanthanides in air atmosphere

E. Y. Ionashiro · F. J. Caires · A. B. Siqueira · L. S. Lima · C. T. Carvalho

Received: 8 April 2011 / Accepted: 11 May 2011 / Published online: 28 May 2011

Abstract Characterization, thermal stability and thermal decomposition of light trivalent lanthanide fumarates, as well as, the thermal behaviour of fumaric acid and its sodium salt were investigated employing simultaneous thermogravimetry and differential thermal analysis, differential scanning calorimetry, Fourier transform infrared spectroscopy (FTIR), TG–FTIR techniques, elemental analysis and complexometry. On heating, sublimation of fumaric acid is observed, while the thermal decomposition of the sodium fumarate occurs with the formation of a mixture of sodium carbonate and carbonaceous residue. The thermal decomposition of light trivalent lanthanide fumarates occurs in consecutive and/or overlapping steps with the formation of the respective oxides: CeO_2, Pr_6O_{11}, and Ln_2O_3 (Ln = La, Nd, Sm, Eu, Gd).

Keywords Fumaric acid · Light lanthanides · Fumarate · Thermal behaviour

E. Y. Ionashiro (✉)
Instituto de Química, UFG, Campus II, Goiania, GO 74001-979, Brazil
e-mail: eyionashiro@hotmail.com

F. J. Caires · L. S. Lima
Instituto de Química, UNESP, CP 355, Araraquara, SP 14801-970, Brazil

A. B. Siqueira
Instituto de Ciências Exatas e da Terra, UFMT, Campus Pontal do Araguaia, Pontal do Araguaia, MT 78698-000, Brazil

C. T. Carvalho
Universidade Federal da Grande Dourados, CEP 79, Dourados, MS 804-970, Brazil

Introduction

Fumaric acid or butenedioic acid, as well as its isomer maleic acid have been used in production of synthetic resins, paper glue, elastomer additives and in the polymer production [1–3]. A literature survey shows that there are interests in the research of coordination compounds from fumaric acid in the production of synthetic polymers and in the production of 3D framework structure [4, 5].

Preparation of some metal-ion compounds of fumarate have been investigated in the solid-state using thermoanalytical techniques in a static atmosphere, X-ray powder diffractometry and infrared spectroscopy. The papers published concern with the thermal decomposition of the compounds: nickel fumarate [6], gadolinium and ytterbium fumarate and succinate [7, 8], comparative study of the thermal analyses of some transition metal(II) maleates and fumarates [9], thermal studies on fumaric acid and crotonic acid compounds of cobalt(II) and nickel(II) [10] and the thermal decomposition reactions of copper(II) maleate and of copper(II) fumarate.

The objective of this research was to prepare solid-state compounds of light trivalent lanthanide succinates (La to Gd, except Pm) to characterize and to investigate by complexometry, elemental analysis, infrared spectroscopy, simultaneous thermogravimetry and differential thermal analysis (TG–DTA), differential scanning calorimetry (DSC) and TG-FTIR techniques. The thermal studies were performed in dynamical dried air atmosphere.

Experimental

Fumaric acid ($C_4H_6O_4$) and sodium fumarate ($Na_2C_4H_4O_4$) both 98% purity were obtained from Sigma. 0.1 mol L^{-1}

aqueous solution of $Na_2C_4H_4O_4$ was prepared by direct weighing of the salt.

Lanthanide chlorides were prepared from the corresponding metal oxides (except for cerium) by treatment with concentrated hydrochloric acid. The resulting solutions were evaporated close to dryness, the residues redissolved in distilled water, and the solution again evaporated close to dryness to eliminate the excess of hydrochloric acid. The residues were again dissolved in distilled water, transferred to a volumetric flask and diluted in order to obtain ca 0.10 mol L^{-1} solutions, whose pH were adjusted to 5.0 using a PH meter with a glass electrode and by adding diluted sodium hydroxide or hydrochloric acid solutions. Cerium(III) was used as its nitrate and ca 0.10 mol L^{-1} aqueous solutions of this ion was prepared by direct weighing of the salt.

The solid-state compounds were prepared by slowly adding, with continuous stirring, the solution of the ligand to the respective metal chloride or nitrate solution, until total precipitation of the metal ions was obtained. The precipitates were washed with distilled water until elimination of the chloride (or nitrate) ions, filtered through and dried on Whatman no. 40 filter paper and kept in a desiccator over anhydrous calcium chloride.

In the solid-state compounds, hydration water, fumarate and metal ions contents were determined from the TG curves. The metal ions were also determined by complexometric titrations with standard EDTA solution, using xylenol orange as indicator [11]. Carbon and hydrogen elemental analysis were performed using an EA 1110, CHNS-O Elemental Analyser (CE Instruments).

The diffuse reflectance infrared spectra of sodium fumarate, as well as for its metal-ion compounds were run on a Nicolet iS10 FT–IR spectrophotometer, using an ATR accessory with Ge window.

Simultaneous TG–DTA and DSC curves were obtained with two thermal analysis systems, model SDT 2960 and DSC Q10, both from TA Instruments. The purge gas was air with flow rate of 100 mL min^{-1} for TG–DTA and 50 mL min^{-1} for DSC experiments. A heating rate of 10 °C min^{-1} was adopted, with samples weighing about 4.000 mg for TG–DTA and about 3.000 mg for DSC runs. Alumina and aluminium crucibles, the latter with perforated cover, were used for TG–DTA and DSC, respectively.

The analyses of the evolved gaseous products were carried out using a Thermogravimetric Analyser Mettler TG–DTA coupled to a FTIR spectrophotometer Nicolet with gas cell and DTGS KBr detector. The furnace and the heated gas cell (250 °C) were coupled through a heated ($T = 200$ °C) 120 cm stainless steel line transfer with 3 mm diameter both purged with dry air (50 mL min^{-1}). The FTIR spectra were recorded with 32 scans per spectrum at a resolution of 4 cm^{-1}.

Results and discussion

The TG–DTA curves of fumaric acid and FTIR spectrum of the material condensed during the heating are shown in Fig. 1a, b. The TG curve shows mass loss in a single step between 190 and 280 °C, corresponding to an endothermic peak at 275 °C (DTA), attributed to the fusion/evaporation of the fumaric acid. This event, which is followed by condensation of the compound, was observed when sample of fumaric acid was heated in a tube glass. The condensed material was identified by infrared spectrum as fumaric acid (Fig. 1b).

The disagreement observed between the TG–DTA profiles, as well as the temperatures of mass loss (TG) and thermal event (DTA), undoubtedly were due to the experimental conditions that were not the same, principally the static air atmosphere that was used in the reference [10], while dynamic air-dried air atmosphere was used in this study.

The sodium fumarate TG–DTA curves, Fig. 2a, show mass losses in two steps between 440–490 and 490–550 °C, corresponding to a large exothermic peak, followed by a small exothermic one, with losses of 30.08 and 2.31%, attributed to the oxidation of the organic matter and of the carbonaceous residue, respectively. The total mass loss up to 550 °C suggests the formation of sodium carbonate (Calcd. = 33.77%, TG = 32.39%). It was observed evaluation of CO_2 in test using hydrochloric acid solution on the

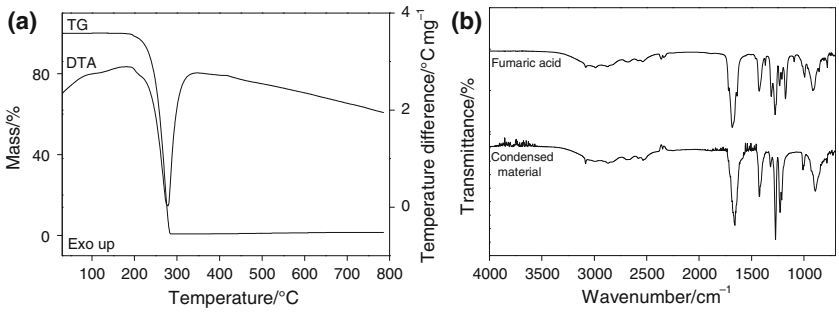

Fig. 1 **a** TG–DTA curves of the fumaric acid (4.432 mg) and **b** FTIR spectrum of the fumaric acid and condensed material

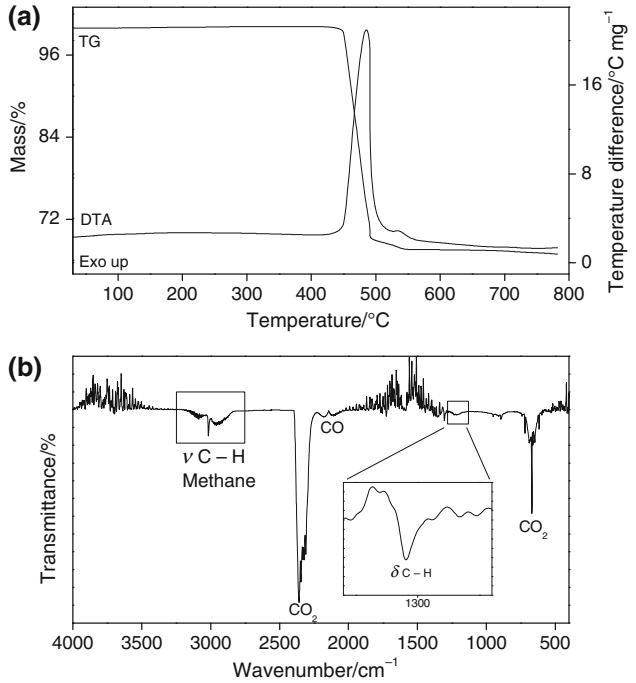

Fig. 2 **a** Simultaneous TG–DTA curves of the sodium fumarate (7.291 mg) and **b** FTIR spectrum of the gaseous products released during the thermal decomposition of the sodium fumarate

residue of the TG curve heated up to 550 °C, confirming the presence of sodium carbonate together with insoluble carbonaceous residue.

The gaseous products evolved during the thermal decomposition of the sodium fumarate were monitored by FTIR and it has carbon dioxide and methane, as the main products. The IR spectrum of the evolved gaseous products is shown in Fig. 2b.

The analytical and thermoanalytical results for the synthesized compounds are shown in Table 1. These results permitted to establish the stoichiometry of the compounds, which are in agreement with the general formula $Ln_2L_3{\cdot}nH_2O$, where Ln represents lanthanides, L is fumarate and $n = 5$ (Sm, Eu), 6 (La to Nd), 6.5 (Gd).

Table 2 Infrared spectroscopic data for sodium fumarate and its compounds with light trivalent lanthanides

Compound	Band position/cm^{-1}			
	ν_{O-H} H_2O/m	$\nu_{as/COO}$/s	$\nu_{sym/COO}$/m	$\Delta\nu/\nu_{as}-\nu_{sym}$
$Na_2(L)$	–	1571	1402	169
$La_2(L)_3{\cdot}6H_2O$	3464	1523	1407	116
$Ce_2(L)_3{\cdot}6H_2O$	3459	1523	1408	115
$Pr_2(L)_3{\cdot}6H_2O$	3454	1522	1409	114
$Nd_2(L){\cdot}6H_2O$	3457	1522	1410	113
$Sm_2(L)_3{\cdot}5H_2O$	3440	1523	1411	113
$Eu_2(L)_3{\cdot}5H_2O$	3261	1532	1397	129
$Gd_2(L)_3{\cdot}6.5H_2O$	3322	1531	1401	130

L fumarate, *m* medium, *s* strong, ν_{O-H} hydroxyl group stretching frequency, $\nu_{as(COO)}$ and $\nu_{sym(COO)}$ anti-symmetrical and symmetrical vibrations of the COO group, respectively

Infrared spectroscopic data on fumarate and its compounds with the lanthanide ions considered in this study are shown in Table 2. The investigation was focused mainly in the 1700–1400 cm^{-1} range because this region is potentially the most informative in attempting to assign coordination sites.

In sodium fumarate, strong band at 1571 cm^{-1} and a medium intensity band located at 1402 cm^{-1} are attributed to the anti-symmetrical and symmetrical frequencies of the carboxylate groups, respectively [12, 13]. For the synthesized compounds, the anti-symmetrical and symmetrical stretching frequencies are located between 1532–1522 and 1411–1397 cm^{-1}, respectively. Analysis of the frequencies of the $\nu_{as(COO)}$ and $\nu_{sym(COO)}$ bands show that the lanthanides are linked to the carboxylate groups by a bidentate bond with an incomplete equalization of the bond lengths in the carboxylate anion, which is an agreement with the literature [14, 15].

The simultaneous TG–DTA curves of the compounds are shown in Fig. 3. These curves show mass losses in two (Ce), three (Sm), four (La, Pr, Eu and Gd) and five (Nd)

Table 1 Analytical data for $Ln_2(L)_3{\cdot}nH_2O$ compounds

Compound	Lanthanide oxide/%			L (lost)/%		H_2O/%		C/%		H/%		Residue
	Calcd.	TG	EDTA	Calcd.	TG	Calcd.	TG	Calcd.	E. A.	Calcd.	E. A.	
$La_2(L)_3{\cdot}6H_2O$	44.75	44.25	44.60	40.40	40.73	14.85	15.02	19.79	19.60	2.50	2.37	La_2O_3
$Ce_2(L)_3{\cdot}6H_2O$	47.12	47.55	47.32	38.08	37.56	14.80	14.89	19.73	19.46	2.49	2.67	CeO_2
$Pr_2(L)_3{\cdot}6H_2O$	46.51	46.57	46.09	38.72	38.65	14.77	14.78	19.69	19.55	2.48	2.27	Pr_6O_{11}
$Nd_2(L)_3{\cdot}6H_2O$	45.55	45.40	45.62	39.82	40.13	14.63	14.47	19.50	19.66	2.46	2.44	Nd_2O_3
$Sm_2(L)_3{\cdot}5H_2O$	47.57	47.43	47.23	40.17	39.83	12.29	12.74	19.66	19.82	2.20	2.08	Sm_2O_3
$Eu_2(L)_3{\cdot}5H_2O$	47.81	47.80	47.61	39.96	39.81	12.24	12.39	19.57	19.65	2.19	2.28	Eu_2O_3
$Gd_2(L)_3{\cdot}6.5H_2O$	46.49	46.86	46.62	38.49	39.87	15.02	15.24	18.48	18.77	2.46	2.50	Gd_2O_3

Ln lanthanides, *L* fumarate, *E. A.* elemental analysis

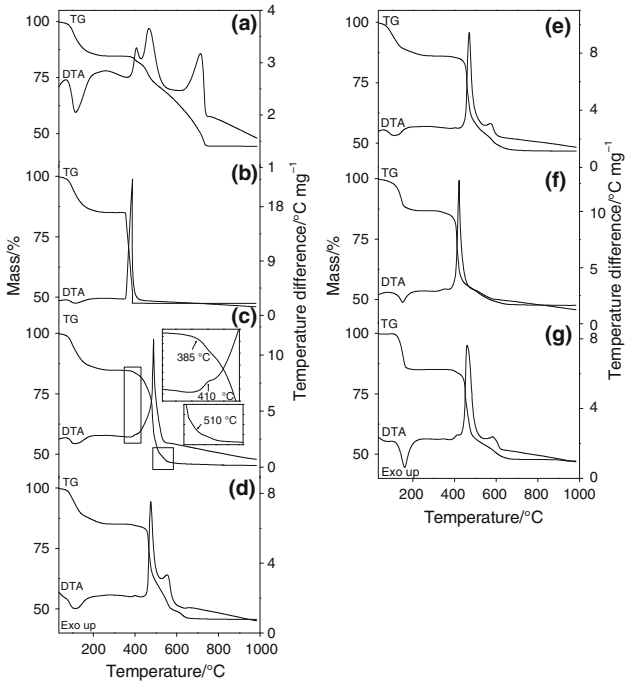

Fig. 3 Simultaneous TG–DTA curves of the compounds: (*a*) $La_2L_3{\cdot}6H_2O$ (4.025 mg); (*b*) $Ce_2L_3{\cdot}5H_2O$ (4.134 mg); (*c*) $Pr_2L_3{\cdot}6H_2O$ (4.071 mg); (*d*) $Nd_2L_3{\cdot}6H_2O$ (4.196 mg); (*e*) $Sm_2L_3{\cdot}5H_2O$ (4.024 mg); (*f*) $Eu_2L_3{\cdot}5H_2O$ (4.024 mg) and (*g*) $Gd_2L_3{\cdot}6.5H_2O$ (4.137 mg)

consecutive and/or overlapping steps and thermal events corresponding to these losses.

For all the compounds, the first mass loss associated to an endothermic DTA peak is ascribed to the dehydration that occurs in a single step in a slow process, except for gadolinium compound, which also occurs in a single step, but through a fast process. The similarity of the TG–DTA curves up to this point suggests that the dehydration mechanism is the same for these compounds.

Once dehydrated, a close similarity is observed concerning the TG–DTA profiles of praseodymium and europium compounds, Fig. 3c, f, and the same for neodymium and gadolinium ones, Fig. 3d, g. On the other hand, lanthanum, cerium and samarium, Fig. 3a–c, display other TG–DTA profiles, characteristic of each compound.

Thus, the features of each of these compounds are discussed on the base of their similar thermal profiles after the dehydration.

Lanthanum compound

The simultaneous TG–DTA curves are shown in Fig. 3a. The first mass observed between 40 and 215 °C, corresponding to an endothermic peak at 115 °C (DTA) is due to dehydration; it reflects the loss of 6 H_2O (Calcd. = 14.85%, TG = 15.02%). The anhydrous compound is stable up to 380 °C, and above this temperature the thermal decomposition occurs in three overlapping steps between 380–430, 430–490 and 490–740 °C, with losses of 3.19, 10.38 and 27.16%, respectively, corresponding to the exothermic DTA peaks at 410, 470 and 710 °C, which are attributed to oxidation of the organic matter. The total mass loss up to 740 °C is in agreement with the formation of La_2O_3, as final residue (Calcd. = 55.25%, TG = 55.75%).

Cerium compound

The simultaneous TG–DTA curves are shown in Fig. 3b. The first mass loss between 40 and 235 °C, corresponding to the endothermic peak at 110 °C in DTA, is due to the dehydration with loss of 6 H_2O (Calcd. = 14.80%, TG = 14.89%). The anhydrous compound is stable up to 350 °C and above this temperature the thermal decomposition occurs in a single step between 350 and 390 °C, with loss of 37.56%, corresponding to the exothermic peak at 390 °C. The less thermal stability of Cerium compound and the exothermic peak at 390 °C are attributed to the oxidation reaction of Ce(III) to Ce(IV), together with the oxidation of the organic matter. This behaviour concerning to the thermal stability of the cerium compound has already been observed for other cerium compounds [16, 17]. The total mass loss up to 390 °C is in agreement with the formation of CeO_2, as final residue (Calcd. = 52.88%, TG = 52.45%).

Praseodymium and europium compounds

The simultaneous TG–DTA curves are shown in Fig. 3c, f, respectively. The first mass loss between 40–245 °C (Pr) and 40–215 °C (Eu), corresponding to an endothermic DTA peak at 110 °C (Pr) and 155 °C (Eu), is due to dehydration with loss of 6 H_2O (Pr) and 5 H_2O (Eu) (Calcd. = 14.77%, TG = 14.78% (Pr); Calcd. = 12.24%, TG = 12.39% (Eu)). The anhydrous compounds are stable up to 385 and 320 °C, respectively, and above this temperature the thermal decomposition occurs in three overlapping steps between 385–410, 410–510 and 510–600 °C (Pr) and 320–375, 375–450 and 450–680 °C (Eu), with losses of 1.20, 32.97 and 4.48% (Pr) and 1.20, 28.44 and 10.17% (Eu), corresponding to exothermic peaks at 400 and 485 °C (Pr) and 355 and 425 °C (Eu) (in DTA), which are attributed to oxidation of the organic matter and for praseodymium compound also the oxidation of Pr(III) to Pr_6O_{11}. The total mass loss up 600 °C (Pr) and 680 °C (Eu) are in agreement with the formation of Pr_6O_{11} and Eu_2O_3, as final residues (Calcd. = 53.49%, TG = 53.43% (Pr); Calcd. = 52.19%, TG = 52.20% (Eu)).

For both compounds, no thermal event corresponding to the last step of mass loss is observed in DTA curve, probably because the net heat in this step is insufficient to produce a thermal event.

Samarium compound

The simultaneous TG–DTA curves are shown in Fig. 3e. The first mass loss between 40 and 245 °C corresponding to an endothermic DTA peak at 115 °C in DTA is due to dehydration with loss of 5 H_2O (Calcd. = 12.29%, TG = 12.74%). Once dehydrated, the compound is stable up to 380 °C and the thermal decomposition occurs in two overlapping steps between 380–540 and 540–670 °C, with losses of 32.41 and 7.42%, corresponding to the exothermic peaks at 470 and 575 °C, attributed to oxidation of the organic matter.

The total mass loss up to 670 °C is in agreement with the formation of Sm_2O_3, as final residue (Calcd. = 52.43%, TG = 52.57%).

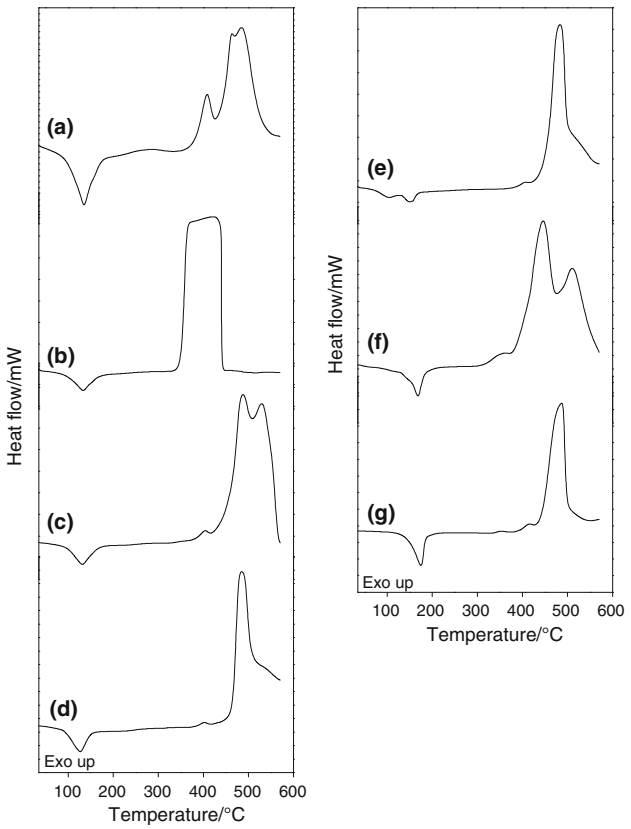

Fig. 4 DSC curves of the compounds: (*a*) $La_2L_3{\cdot}6H_2O$ (3.198 mg); (*b*) $Ce_2L_3{\cdot}6H_2O$ (3.122 mg); (*c*) $Pr_2L_3{\cdot}6H_2O$ (3.353 mg); (*d*) $Nd_2L_3{\cdot}6H_2O$ (2.997 mg); (*e*) $Sm_2L_3{\cdot}5H_2O$ (3.097 mg); (*f*) $Eu_2L_3{\cdot}5H_2O$ (3.311 mg) and (*g*) $Gd_2L_3{\cdot}6.5H_2O$ (3.259 mg)

Neodymium and gadolinium compounds

The simultaneous TG–DTA curves are shown in Fig. 3d, g, respectively. The first mass loss between 40–250 °C (Nd) and 105–210 °C (Gd) corresponding to an endothermic peak at 110 and 160 °C, respectively, is due to dehydration with loss 6 H_2O (Nd) and 6.5 H_2O (Gd) (Calcd. = 14.63%, TG = 14.47% (Nd); Calcd. = 15.02%, TG = 15.24% (Gd)). The anhydrous compounds are stable up to 385 °C and above this temperature the thermal decomposition occurs in three (Gd) or four (Nd) consecutive and/or overlapping steps between 385–430, 430–520, 520–580 and 580–660 °C (Nd) or 385–430, 430–525 and 525–670 °C (Gd), with losses of 1.20, 22.36, 12.38 and 4.19% (Nd) or 2.39, 26.73 and 8.78% (Gd), corresponding to exothermic peaks at 400, 480 and 560 °C (Nd) or 410, 460 and 585 °C (Gd) in DTA, which are attributed to oxidation of the organic matter. The endothermic peak at 640 °C corresponding to the last mass loss observed only in the neodymium compound is attributed to the thermal decomposition of the dioxycarbonate formed as intermediate. The total mass loss up to 660 °C (Nd) and 670 °C (Gd) are in agreement with the formation of Nd_2O_3 and Gd_2O_3, as final residues (Calcd. = 54.45%, TG = 54.60% (Nd); Calcd. = 53.51%, TG = 53.14% (Gd)).

The DSC curves of the compounds are shown in Fig. 4. These curves show endothermic and exothermic peaks that are in full agreement with the thermal events observed in the DTA curves. The endothermic peaks at 136 °C (La), 134 °C (Ce), 131 °C (Pr), 127 °C (Nd), 105 and 151 °C (Sm), 169 °C (Eu) and 175 °C (Gd) are attributed to the dehydration. The dehydration enthalpies found for these compounds were: 214 (La), 196 (Ce), 199 (Pr), 177 (Nd), 38 and 58 (Sm), 244 (Eu) and 308 (Gd) kJ mol^{-1}. In all the

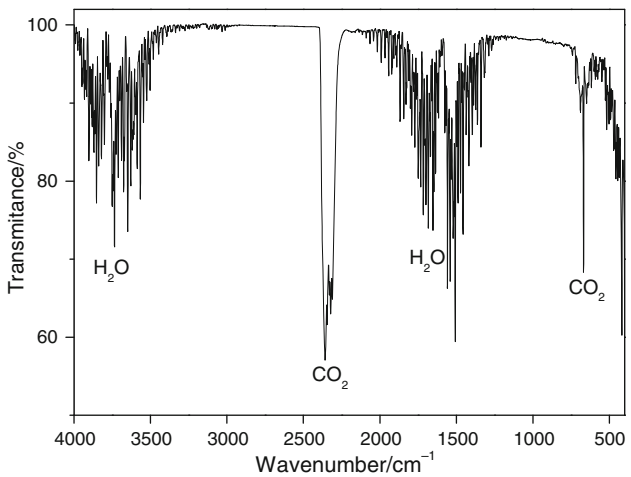

Fig. 5 FTIR spectrum of the gases released during the decomposition of the lanthanum fumarate, as representative of all the lanthanide compounds

compounds, the thermal events above 330 °C are due to the thermal decomposition, where the oxidation of the organic matter occurs in consecutive and/or overlapping steps.

The gaseous products evolved during the thermal decomposition of the light lanthanide fumarates were monitored by FTIR and it has carbon dioxide (anti-symmetrical stretching in 2360 and 2345 and scissoring (degenerated) in 666 cm^{-1}) and water as main products due to the decarboxylation and oxidation of the organic matter. The FTIR spectra of the gaseous products evolved during the thermal decomposition of lanthanum fumarate, as representative of all these compounds, are shown in Fig. 5.

Conclusions

From TG, complexometry and elemental analysis data, a general formula could be established for these compounds in the solid-state. All the compounds in this series dehydrate in a single step.

The gaseous products evolved during the thermal decomposition of the sodium fumarate were carbon monoxide, carbon dioxide and methane, while for the light lanthanide fumarates have carbon dioxide and water as main products.

The reflectance infrared spectroscopic data suggests that the lanthanides are linked to carboxylate groups by a bidentate bonding with an incomplete equalization of the bonding lengths in the carboxylate anion.

The TG–DTA and DSC curves provided previously unreported information about the thermal stability and thermal decomposition of these compounds.

The anhydrous stability series for the studied compounds are: Nd (320 °C), Ce (350 °C), La (380 °C), Sm (380 °C), Pr (380 °C), Eu (385 °C) and Gd (385 °C). The Dehydration stability series for the studied compounds are: Gd (210 °C), La (215 °C), Nd (215 °C), Ce (235 °C), Pr (245 °C), Sm (245 °C) and Eu (250 °C).

Acknowledgements The author thanks FAPESP, CNPQ Edital Universal and CAPES Brazilian agencies for financial support.

References

1. Jansen J, Melchels Ferry PW, Grijpma DW, Feijen J. Acid monoethyl esther-functionalized poly(D, L-lactide)/*N*-vinyl-2-pyrrolidone resins for the preparation of tissue engineering scaffolds by stereolithography. Biomacromolecules. 2009;10:214–20.
2. Aleksandrovic V, Djonlagic J. Synthesis and characterization of thermoplastic copolyester elastomers modified with fumaric moieties. J Serb Chem Soc. 2001;66:139–52.
3. Ohnishi M, Uno T, Kubo M, Itoh T. Synthesis and radical polymerization of dissymmetric fumarates with alkoxyethyl, bulky siloxy groups. J Polym Sci A Polym Chem. 2009;47:420–33.
4. Zhu WH, Wang ZM, Gao S. Two 3D porous lanthanide–fumarate–oxalate frameworks exhibiting framework dynamics and luminescent change upon reversible de- and rehydration. Inorg Chem. 2007;46:1337–42.
5. Zhu WH, Wang ZM, Gao S. A 3D porous lanthanide–fumarate framework with water hexamer occupied cavities, exhibiting a reversible dehydration and rehydration procedure. Dalton Trans. 2003;6:765–8.
6. Mac Ginn MJ, Wheeler BR, Galwey AK. Thermal decomposition of nickel fumarate. Trans Faraday Soc. 1970;66:1809–16.
7. Sevost'yanov VP, Dvornikova LM. Thermal decomposition of gadolinium fumarate and succinate. Izv Vyss Uchebn Zaved Khim Khim Tekhnol. 1971;14:1771–3.
8. Sevost'yanov VP, Dvornikova LM. Thermal decomposition of ytterbium fumarate and succinate. Zhur Neorg Khim. 1972;17:2884–7.
9. Bassi PS, Randhawa BS, Khajuria CM, Kaur S. Comparative study of the thermal analyses of some transition metal(II) maleates and fumarates. J Therm Anal. 1987;32:569–77.
10. Allan JR, Bonner JG, Bowley HJ, Gerrard DL, Hoey S. Thermal studies on fumaric acid and crotonic acid compounds of cobalt(II) and nickel(II). Thermochim Acta. 1989;141:227–33.
11. Ionashiro M, Graner CAF, Zuanon Netto J. Complexometric titration of lanthanides and yttrium. Ecl Quim. 1983;8:29–32.
12. Socrates G. Infrared characteristic group frequencies. 2nd ed. New York: Wiley; 1994. p. 91, 236–7.
13. Silverstein RM, Webster FX. Spectrometric identification of organic compounds. 6th ed. New York: Wiley; 1998. p. 92, 93, 96, 97.
14. Lewandowski W, Baranska H. Vibrational and electronic spectroscopic study of lanthanides and effect of sodium on the aromatic system of benzoic acid. J Raman Spectrosc. 1986;17:17–22.
15. Siqueira AB, Carvalho CT, Ionashiro EY, Bannach G, Rodrigues EC, Ionashiro M. Synthesis, characterization and thermal behaviour of solid 2-methoxybenzoates of trivalent metals. J Therm Anal Calorim. 2008;98:945–51.
16. Locatelli JR, Rodrigues EC, Siqueira AB, Ionashiro EY, Bannach G, Ionashiro M. Synthesis, characterization and thermal behaviour of solid-state compounds of yttrium and lanthanide benzoates. J Ther Anal Calorim. 2007;90:737–46.
17. Siqueira AB, Bannach G, Rodrigues EC, Carvalho CT, Ionashiro M. Solid-state 2-methoxybenzoates of light trivalent lanthanides. Synthesis, characterization and thermal behaviour. J Therm Anal Calorim. 2008;91:897–902.